

# An Analytical Model for Predicting the Underfill Flow Characteristics in Flip-Chip Encapsulation

J. W. Wan, W. J. Zhang, *Member, IEEE*, and D. J. Bergstrom

**Abstract**—This article describes an analytical model for the prediction of the underfill flow characteristics in a flip-chip package driven by capillary action. In this model, we consider non-Newtonian fluid properties of the encapsulant as opposed to most other studies where Newtonian fluid properties were assumed for the underfill flow. The power-law constitutive equation was applied in our study. The simulation based on this model agreed well with the measurement obtained from the experiments available in literature. It was further shown that this model performs better than the Washburn model traditionally used for the prediction of underfill flow characteristics in the flip-chip packaging. Based on this model, the effects of the solder bump pattern (including bump pitch, solder bump diameter, and gap height) on the process variables (i.e., flow front and filling time) were studied, which facilitated both the package design and the process optimization.

**Index Terms**—Analytical model, flip-chip package, power-law constitutive equation, surface tension, underfill flow, Washburn model.

## I. INTRODUCTION

**B**ECAUSE of the evolution of the integrated circuit and the desire for higher performance and lower cost, flip-chip technology has become more attractive to the electronics packaging industry. Flip-chip technology has advantages over other methods as it increases the packaging density and improves the electrical performance with lower cost. Traditionally, this technology uses ceramic materials for the substrate. Because of the similarity in the thermal expansion coefficient (CTE) of the chip and the ceramic substrate, i.e., there is only a small mismatch in CTEs between the chip and the substrate, the amount of stress on the solder joint produced by this mismatch is relatively small. Unless a very large chip is involved, the deformation of the joint is small and within safe limits. The desire for further cost reduction and increase in production volume has resulted in the use of organic materials. As a negative consequence of this, the difference in CTEs between the silicon chip (about 2.3 ppm/°C) and the organic substrate (18–25 ppm/°C) can cause significant thermal stresses on the interconnects during temperature cycling, which have contributed to fracture of the solder joint in practice. One method used at present to solve this problem is to fill an appropriate encapsulant into the gap between the chip and the substrate to redistribute the shear stresses originally concentrated on the solder joint to the die and the substrate.

Manuscript received May 22, 2003; revised July 22, 2004, November 18, 2004. This work was supported in part by the NSERC Discovery Grant.

The authors are with the Department of Mechanical Engineering, University of Saskatchewan, Saskatoon, SK S7N 5A9, Canada (e-mail: wjz485@Engr.Usask.Ca).

Digital Object Identifier 10.1109/TADVP.2005.848385

Currently, most flip-chips are encapsulated by dispensing the encapsulant along the periphery of one or two sides of the chip. Capillary action (i.e., surface tension) drives the encapsulant to flow through the microcavity formed between the chip and the substrate. After filling is complete, the chip and substrate assembly are taken to an oven where the underfill is cured. The underfilling process needs to be controlled to achieve a satisfactory result, and is measured by two performance indices: 1) the flow front and 2) the time needed for the fluid to completely fill the cavity.

A computationally effective model that relates these indexes to both process and design parameters would be helpful for process optimization and control. Ideally, such a model would be in analytical form with a closed-form solution. Studies on modeling the flow behavior of the underfill in the flip-chip application have been performed by others [1]–[5], [7]–[11]. These studies can be classified in terms of as follows:

- 1) the type of fluid considered for the underfill materials (Newtonian, non-Newtonian);
- 2) the physical geometry of the confining walls (two parallel plates, two parallel plates with the presence of an array of solder bumps);
- 3) the type of model (analytical form, numerical form, e.g., finite element technology).

In the studies reported in [1]–[5], [11], the Washburn model [6] for the case of two parallel plates was applied. The model assumes that the underfill is laminar, one dimensional, incompressible, and fully developed flow of a Newtonian fluid. The application of the Washburn model leads to the following equation for the flow front:

$$x_f^2 = \frac{\sigma h \cos \theta}{3\eta} t \quad (1)$$

where  $\sigma$  is the surface tension,  $x_f$  the position of the flow-front at time  $t$ ,  $\theta$  the contact angle,  $\eta$  the viscosity, and  $h$  the thickness of the cavity (see Fig. 1). From (1), the filling time  $t_f$  of encapsulation is

$$t_f = \frac{3\eta L^2}{\sigma h \cos \theta} \quad (2)$$

where  $L$  is the length of the cavity.

Unfortunately, the filling time calculated with the above equation does not agree well with experimental data [3], [4], [9]. This is because the Washburn model is primarily for Newtonian fluids, while underfill materials for flip-chip packaging exhibit non-Newtonian fluid behavior [4], [7]–[9]. In the study presented by Han and Wang [4], the contact angle  $\theta$  was considered to vary with respect to time as a modification of

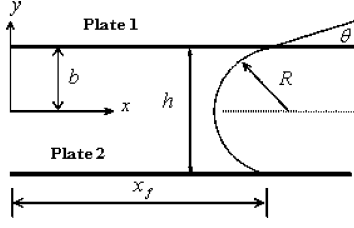


Fig. 1. Underfill flow between two parallel plates.

the Washburn model. In particular, they employed the equation for the time-varying (or dynamic) contact angle of Newman [16]. While acknowledging that the dynamic contact angle does relate to the flow of polymer melts [17], the non-Newtonian behavior of the fluid was not explicitly represented. Han and Wang [4] further implied that their analytical model was primarily for a Newtonian fluid, and went on to develop a numerical model using a generalized Hele–Shaw model. While a numerical model is conducive to understanding the physics of the underfill process, it is not in line with the main objective as well as the scope of the present study, i.e., a computation-effective model for process optimization and control. A comprehensive study including both simulation and experiment was reported by Nguyen *et al.* [7]. However, their model for simulation was also a numerical one and ignored the feature of viscosity change with respect to time and shear rate. It is of interest to know what computational resources are needed in order to complete one simulation using a numerical approach in a flip-chip package. Gordon *et al.* [11] reported that it took 10 days of run time on a Sparc20 workstation by Flunt software to complete one simulation using the Hele–Shaw model. Our experience in using Ansys to simulate a two-dimensional (2-D) underfill process is such that the simulation takes more than 10 h with a Pentium 4 personal computer.

The objective of the study presented in this paper was to develop a computation-effective (or a lumped parameter analytical) model for the underfill flow process, which specifically considers that the underfill material is a non-Newtonian fluid and the resistance caused by solder bump affects the flow of filling material. The analytical model developed was verified with the experimental data produced by Nguyen *et al.* [7] and Fine *et al.* [8].

## II. THE NON-NEWTONIAN UNDERFILL FLOW ANALYSIS

The underfill flow driven by capillary action is a relatively slow process. It can be assumed that such a flow is laminar, fully developed, and incompressible. Under these assumptions, the momentum equation of the flow can be simplified as [12]

$$0 = -[\nabla \cdot \boldsymbol{\tau}] - \nabla p \quad (3)$$

where  $\boldsymbol{\tau}$  is the stress tensor, and  $p$  is the pressure. Considering that the flow is 2-D in  $x$  and  $y$ , (3) reduces to

$$\frac{\partial \tau_{xy}}{\partial y} = -\frac{\partial p}{\partial x}. \quad (4)$$

The well-known power-law model [13] is adopted as the constitutive equation, i.e.,

$$\tau_{xy} = m |II_{2D}|^{(n-1)/2} (2D_{xy}) \quad (5)$$

where  $D$  is the rate of deformation tensor, and  $II_{2D}$  is the second invariant of  $D$ . For a steady simple shear flow,  $|II_{2D}| = \dot{\gamma}^2$  and  $2D_{xy} = du/dy$  [13]. Equation (5) becomes

$$\tau_{xy} = m \dot{\gamma}^{n-1} \frac{du}{dy} \quad (6)$$

where,  $\dot{\gamma} = du/dy$  is the shear rate,  $m$  and  $n$  are constants depending on the temperature, and  $u$  is the velocity of the flow in the  $x$  direction. The apparent viscosity  $\eta$  of the fluid can be expressed as

$$\eta = m \dot{\gamma}^{n-1}. \quad (7)$$

Substituting (6) and (7) into (4) gives

$$\frac{d}{dy} \left( \eta \frac{du}{dy} \right) = -\frac{dp}{dx}. \quad (8)$$

Integrating (8) subject to the symmetry boundary condition at the centerline, i.e.,  $(du/dy)|_{y=0} = 0$ , gives

$$\eta \frac{du}{dy} = \left( -\frac{dp}{dx} \right) y. \quad (9)$$

Substituting (7) into (9) results in

$$m \left( \frac{du}{dy} \right)^n = \left( -\frac{dp}{dx} \right) y \quad (10)$$

which can be rearranged to obtain

$$\frac{du}{dy} = \left( \frac{-\frac{dp}{dx}}{m} \right)^{1/n} y^{1/n}. \quad (11)$$

Finally, integrating (11) subject to the no-slip boundary condition at the wall, i.e.,  $u|_{y=\pm b} = 0$ , gives the following gap-wise velocity profile:

$$u(y) = \frac{n}{n+1} \left( \frac{-\frac{dp}{dx}}{m} \right)^{1/n} \left( b^{(n+1)/n} - y^{(n+1)/n} \right) \quad (12)$$

where  $b = h/2$ ,  $h$  is the thickness of the gap, and  $dp/dx$  is the pressure gradient. The speed of the flow-front is equal to the average gap-wise velocity, which is given by

$$\bar{u} = \frac{dx_f}{dt} = \frac{1}{b} \int_0^b u dy. \quad (13)$$

Substituting (12) into (13) and integrating gives

$$\frac{dx_f}{dt} = \frac{n}{2n+1} \left( \frac{-\frac{dp}{dx}}{m} \right)^{1/n} b^{(n+1)/n}.$$

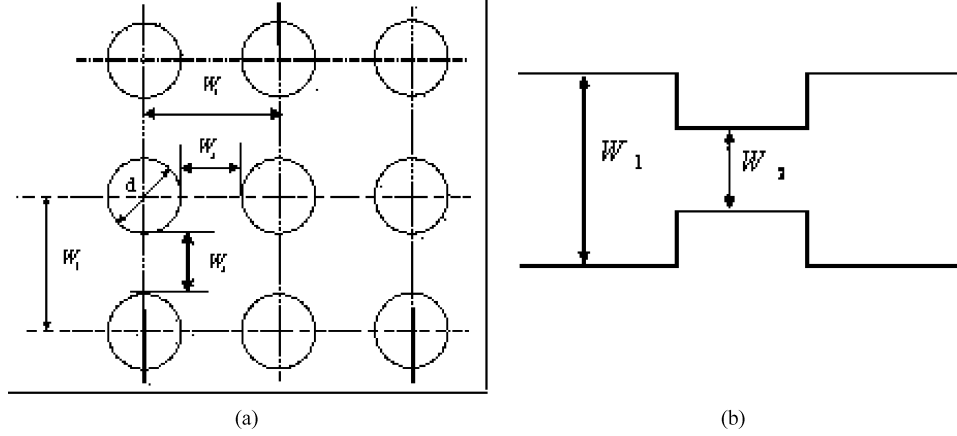


Fig. 2. Flip-chip package pattern. (a) General structure. (b) Generic flow passage.

The above equation can be rearranged to obtain

$$\frac{m \left( \frac{dx_f}{dt} \right)^n}{\left( \frac{n}{2n+1} \right)^n b^{n+1}} = -\frac{dp}{dx}. \quad (14)$$

Since  $dx_f/dt$  is independent of  $x$  and  $dp/dx$  is independent of  $t$ , (14) can be separated into two ordinary differential equations

$$\frac{m \left( \frac{dx_f}{dt} \right)^n}{\left( \frac{n}{2n+1} \right)^n b^{n+1}} = c \quad (15)$$

$$-\frac{dp}{dx} = c \quad (16)$$

where  $c$  is a constant. Integrating (16) and applying the boundary conditions in terms of the external pressure and the pressure at the flow front

$$-\frac{dp}{dx} = \frac{p_0 - p_f}{x_f} = -\frac{\Delta p}{x_f}. \quad (17)$$

Substituting (17) into (14) gives

$$\frac{m \left( \frac{dx_f}{dt} \right)^n}{\left( \frac{n}{2n+1} \right)^n b^{n+1}} = \frac{\Delta p}{x_f}. \quad (18)$$

Integrating the above equation, the flow front is given by

$$x_f = \frac{h}{2} \left( \frac{\Delta p}{m} \right)^{1/(n+1)} \left( \frac{n+1}{2n+1} t \right)^{n/(n+1)}. \quad (19)$$

From the above equation, the filling times is given by the following equation

$$t_f = \frac{2n+1}{n+1} \left( \frac{m}{\Delta p} \right)^{1/n} \left( \frac{2x}{h} \right)^{(n+1)/n} \quad (20)$$

where  $\Delta p$  is the pressure difference due to flow resistance. In the fluid flow between two parallel plates driven by capillary action, the net driving force in this case is the pressure difference due

to surface tension, which can be calculated using the following equation [5]:

$$\Delta p = \frac{\sigma}{R} = \frac{2\sigma \cos \theta}{h} \quad (21)$$

where  $\sigma$  is the surface tension of the fluid in N/m,  $R$  is the radius of curvature of the flow-front, and  $\theta$  is the contact angle (see Fig. 1).

Substituting (21) into (19) and (20), respectively, we obtain

$$x_f = \left( \frac{\sigma \cos \theta}{m} \right)^{1/(n+1)} \left( \frac{(n+1)b}{2n+1} t \right)^{n/(n+1)} \quad (22)$$

$$t_f = \left( \frac{2n+1}{(n+1)b} \right) \left( \frac{m}{\sigma \cos \theta} \right)^{1/n} x^{(n+1)/n}. \quad (23)$$

We can verify that when  $n = 1$ , (22) and (23) reduce to (1) and (2), respectively, which represent the Washburn model.

### III. UNDERFILL FLOW IN FLIP-CHIP PACKAGE

We carried out an experiment based on a flow configuration created by two plates [19]. The model developed above was validated based on the experimental results. However, the simulation based on the model does not give a good prediction in the case of an actual flip-chip package [8], [9]. The observed results for a full array and perimeter array flip-chip pattern reported by Fine *et al.* [8] clearly show that the encapsulant flows faster in the perimeter array than in the full array, and that the solder bumps significantly affect both the flow rate and the uniformity of the flow. In this section, we extend the model for the flip-chip package by considering the effects of solder bumps on the flow.

The effect of solder bumps in this case is an additional resistance to the fluid flow, which can be further represented by the pressure loss ( $\Delta p_j$ ). This means that the driving force, as calculated by (21), will have to be reduced by  $\Delta p_j$ . The full array solder bump pattern, as a generic feature of the flip-chip package, is described in Fig. 2. An array consisting of two rows is a reasonable representative structure [Fig. 2(a)]. Based on the assumption that the underfill flow consists of a set of one-dimensional channel flows, the problem can be further simplified to the approximate geometry shown in Fig. 2(b). For the capillary flow shown in Fig. 2(b), the pressure drop,  $\Delta p_j$ , associated

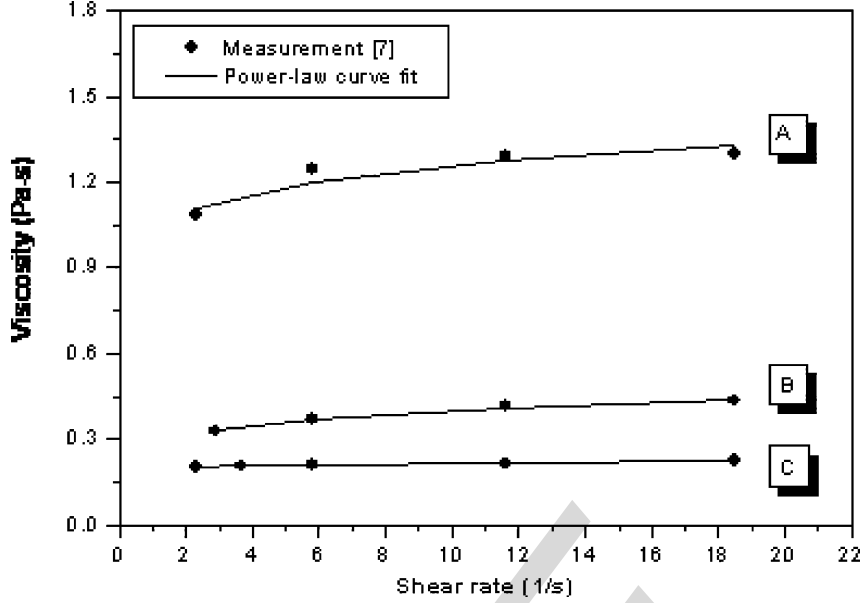


Fig. 3. Power-law models fitted from the measurements reported in [7]. A, B, C: three different materials.

with the variation in cross section between 1 and 2, is given by [14], [15]

$$\Delta p_j = 2\sigma \cos \theta \left[ \left( \frac{1}{W_2} + \frac{1}{h_2} \right) - \left( \frac{1}{W_1} + \frac{1}{h_1} \right) \right]. \quad (24)$$

It should be pointed out that (24), which describes the pressure required to force fluid into or past a restriction, is independent of the length of the restriction [14]. Furthermore, it is interesting to note that it is also independent of the flow rate [14]. When the channel thickness is the same, i.e.,  $h_1 = h_2$ , the above equation becomes

$$\Delta p_j = 2\sigma \cos \theta \left( \frac{1}{W_2} - \frac{1}{W_1} \right). \quad (25)$$

From Fig. 2, we further have

$$W_1 = W_2 + d \quad (26)$$

where  $d$  is the diameter of the solder bump. Substituting (26) into (25) gives

$$\Delta p_j = \frac{2d\sigma \cos \theta}{W_2(W_2 + d)}. \quad (27)$$

According to the previous elaboration, the driving pressure is the pressure due to the surface tension between the chip and the substrate deducted by  $\Delta p_j$ . The driving pressure in this case is given by

$$\Delta p = \frac{2\sigma \cos \theta}{h} - \frac{2d\sigma \cos \theta}{W_2(W_2 + d)}. \quad (28)$$

Equation (28) is further rearranged into the following equation, i.e.,

$$\Delta p = \frac{2\sigma \cos \theta (W_2^2 + dW_2 - dh)}{hW_2(W_2 + d)}. \quad (29)$$

TABLE I  
MEASURED FILLING TIME VERSUS CALCULATED FITTING TIME

Material	A	B	C	
Power-law index $m$	1.03	0.28	0.19	Fitted data
Power-law index $n$	1.09	1.15	1.05	Fitted data
Contact angle (degree)	25.5	20.4	17.5	measured data
Surface tension at 80 °C	0.027	0.027	0.0312	measured data
Filling time (s)	420	60	25	measured data [7]
Filling time (s)	69.1	32.3	13.3	Washburn model
Filling time (s)	201.0	65.2	32.3	Developed analytical model

By substituting (29) into (19) and (20), the flow front and the filling time in the flip-chip package are given by the following equations, respectively:

$$x_f = \frac{h}{2} \left( \frac{2\sigma \cos \theta (W_2^2 + dW_2 - dh)}{mhW(W_2 + d)} \right)^{1/(n+1)} \left( \frac{n+1}{2n+1} t \right)^{n/(n+1)} \quad (30)$$

$$t_f = \frac{2n+1}{n+1} \left( \frac{mhW(W_2 + d)}{2\sigma \cos \theta (W_2^2 + dW_2 - dh)} \right)^{1/n} \left( \frac{2x}{h} \right)^{(n+1)/n} \quad (31)$$

where, for simplicity,  $W_2$  was replaced with  $W$ . We can verify that when  $d = 0$ , the above equations reduce to (22) and (23), i.e., the underfill flow between two parallel plates.

#### IV. MODEL VERIFICATION

Nguyen *et al.* [7] experimentally investigated underfill flow characteristics for various kinds of encapsulant materials. The geometry of their experimental flip-chip package was as follows: the length of the chip is 6.7 mm, the thickness of the cavity is 56  $\mu\text{m}$ , the solder bump pitch is 250  $\mu\text{m}$ , and the clearance between the adjacent solder joints is 82  $\mu\text{m}$ . The measured contact angle, surface tension, and filling time are given in Table I.

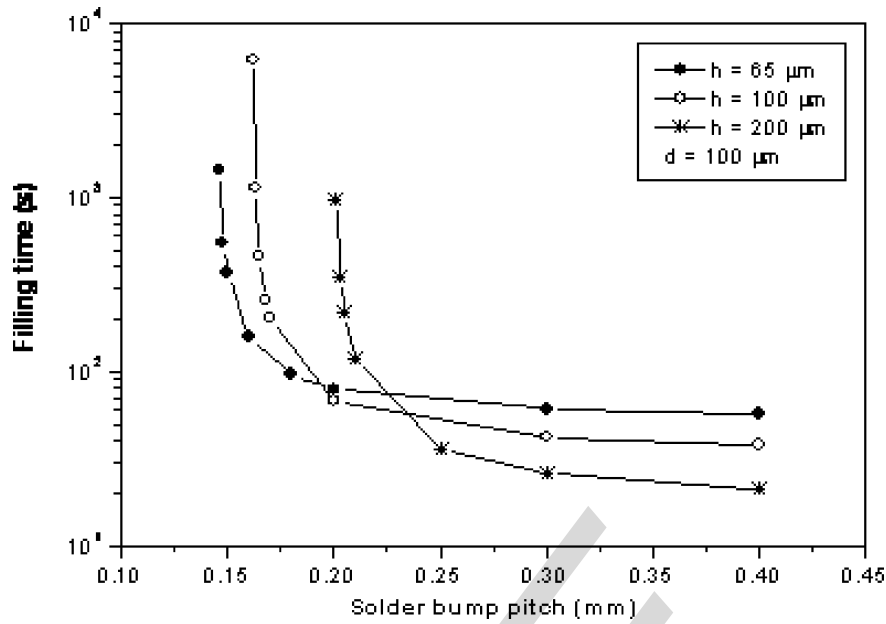


Fig. 4. Effect of the solder bump pitch on the filling time for different gap heights.

Based on their measured viscosities of three different encapsulant materials (A, B, and C), the power-law models were created and are shown in Fig. 3.

The results calculated using the analytical model represented by (31) and using the Washburn model [6], respectively, are listed in Table I for comparison. From a comparison we note that the analytical model gives an adequate prediction of the filling time for materials B and C, but gives a poor prediction for material A. A plausible reason for this could be the time dependency of the viscosity in the case of some non-Newtonian fluids. In particular, the change in the viscosity due to curing may become significant for a long filling process. In all three cases, the predicted results with our model are substantially better than the results calculated with the Washburn model.

Fine *et al.* [8] also experimentally investigated the influence of the solder bump pattern on the filling time. The conditions for the experiment were as follows [8]: the length of the chip is 12.7 mm, the thickness of the cavity is 75  $\mu\text{m}$ , the solder bump pitches are 200  $\mu\text{m}$ , 250  $\mu\text{m}$ , and 400  $\mu\text{m}$ , respectively, the contact angle on the FR4 substrate is 17.5 degree, and the surface tension at 80  $^{\circ}\text{C}$  is 0.0312 N/m. The solder bump diameter was 100  $\mu\text{m}$  for the 200- $\mu\text{m}$  solder bump pitch, and was 125  $\mu\text{m}$  for both the 250- and 400- $\mu\text{m}$  solder bump pitches. Table II shows a comparison of the predicted and the measured filling time with different bump pitches. The produced filling time was again calculated using (31). It can be seen from Table II that the predicted results agree well with the measured results. Both indicate that the filling time decreases with an increase in the pitch distance.

#### V. APPLICATION OF THE MODEL FOR DESIGN AND PROCESS OPTIMIZATION

The influence of the solder bump pattern on filling time is presented in Fig. 4 to Fig. 5. Fig. 4 shows the effect of the bump pitch on the filling time for different gap heights. From these results, we can see that, first, for a fixed solder bump pitch and

TABLE II  
MEASURED FILLING TIME VERSUS CALCULATED FITTING TIME FOR DIFFERENT PITCHES

Bump pitch ( $\mu\text{m}$ )	Measured filling time (s) [8]	Calculated filling time (s) with analytical model	Relative error (%)
200	75	73.2	2.4
250	70	65.7	6.1
400	52	51.0	1.9

solder bump diameter, the filling time decreases with an increase in gap height. This is because the capillary force decreases with an increase of the gap height. Second, for a fixed solder bump diameter, when bump pitch is reduced to a certain value, say 300  $\mu\text{m}$  for the 100- $\mu\text{m}$  gap height, the filling time begins to increase sharply because of the increase in flow resistance caused by the small clearance between the adjacent solder joints. However, when the bump pitch is greater than this value, the influence of bump pitch on filling time becomes very small because of the small flow resistance (due to the large clearance between the adjacent solder joints). This phenomenon agrees with the experimental results reported by Fine *et al.* [8]. They experimentally investigated the influence of different bump pitches, 200, 250, and 400  $\mu\text{m}$ , on filling time with different materials. For all tested materials, they found that the slowest flow occurred for high solder bump density geometry (200  $\mu\text{m}$  pitch), and that when solder bump pitches were increased to 250 and 400  $\mu\text{m}$ , the observed flows became faster. These experimental results show that small solder bump pitches increase flow resistance and cause a longer filling time. A similar phenomenon was also found in the measurements of Gordon *et al.* [11]. In their measurement with a 50- $\mu\text{m}$  gap height, they found that for the full array bumps with a 250- and a 500- $\mu\text{m}$  pitch (174- and 348- $\mu\text{m}$  clearance, respectively), the filling times were nearly the same. This implies that for the flip-chip geometry in their test, the flow resistance caused by the clearance between the adjacent solder

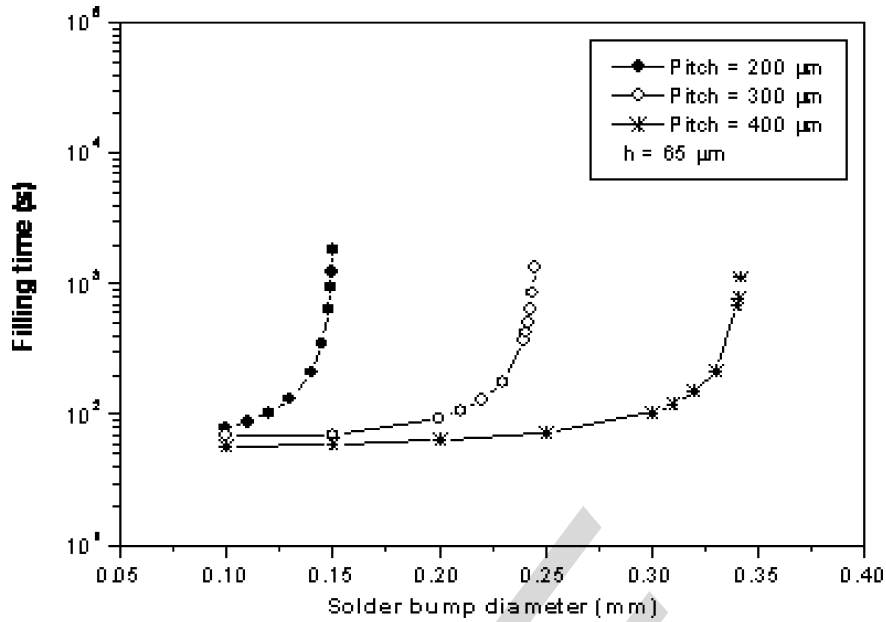


Fig. 5. Effect of the solder bump diameter on the filling time for different solder bump pitches.

joints became very small when bump pitch was larger than 250  $\mu\text{m}$ .

Fig. 5 examines the effect of the solder bump diameter on the filling time for different solder bump pitches. For a fixed solder bump pitch, the filling time increases with the increase of the solder diameter because of the increase of flow resistance caused by the small clearance between the adjacent solder joints. Before the solder bump diameter is increased to a “critical” value, the increase in filling time is relatively small. After the solder diameter increases beyond this critical diameter, the filling time increases very rapidly. We can see that an approximate critical solder bump diameter is about 300  $\mu\text{m}$  for the 400- $\mu\text{m}$  solder bump pitch for the conditions simulated in Fig. 5. These results indicate that the critical solder bump diameter increases with an increase of solder bump pitch. These underfill flow characteristics show that in the design of the solder bump pattern in flip-chip packaging, in order to reduce filling time, the solder diameter should be less than its critical value.

The effect of “critical bump pitch” on filling time was also found by Young and Yang [18]. Their approach was primarily a numerical one. It is noted that their model has the following features.

- 1) The capillary effect between two solder bumps, in addition to the one between the chip and substrate, is considered.
- 2) The pressure gradient between two solder bumps, in addition to the one between the chip and the substrate, is considered, and further, these two pressure gradients generate the same velocity at a point.
- 3) The momentum equation is only suitable for Newtonian fluids.

Based on their model, they observed somewhat the opposite result compared to the result of our model and the experimental results based on the measurement of the experimental system [7], [8] and [11]. Specifically, for the gap height (35  $\mu\text{m}$ ) and the same solder diameter (125  $\mu\text{m}$ ) the filling time for the flip-

chip package with the 400- $\mu\text{m}$  pitch is larger than that with the 200- $\mu\text{m}$  pitch. The possible cause for this disagreement may be some inadequacies in the three features with their model, as previously mentioned. For example, with their second feature, the assumption underlying the Hele–Shaw model, i.e., the thickness of the gap between the two parallel plates should be far less than the width (see comment made by Han and Wang [4]), is no longer valid for the flow between two solder bumps. With respect to their third feature, the classical Hele–Shaw model (only suitable for Newtonian fluids) with the non-Newtonian constitutive equation (i.e., the generalized power-law model) may produce some significant error for non-Newtonian fluids.

## VI. CONCLUSION

In this paper, a computation-effective model for prediction of the flow behavior of non-Newtonian fluids in the context of the flip-chip underfill was developed. The driving force for fluid flow in this case is surface tension. The model was verified by comparison of the simulated results with measured results reported in literature, and was shown to be superior to the Washburn model traditionally used for the underfill flow analysis in flip-chip packaging. The model explicitly correlates the flow behavior with the design parameters in the flip-chip package. Specifically, the following conclusions can be drawn from this study.

- (1) The treatment of underfill materials for the flip-chip package as being Newtonian is not suitable. The materials should be treated as non-Newtonian fluids. In particular, the property that the viscosity of the underfill material changes with respect to the shear rate needs to be represented for most of the underfill processes. The power-law constitutive equation is adequate to represent this property.
- (2) Use of the power-law constitutive equation results in an analytical model for predicting the flow behavior of the

underfill with a closed form solution. This is as opposed to the result obtained by Han and Wang [4], which is based on the Washburn model and consideration of a dynamic contact angle. The solution to their model requires an iterative scheme.

- (3) In the case of the surface tension driven flow of non-Newtonian fluids, the resistance caused by the solder bump pattern cannot be ignored. The flow of the underfill material within the flip-chip package (i.e., two parallel plates with a full array of solder bumps) can be approximated by flow in multiple channels.
- (4) The design parameters, namely: the gap height, the bump pitch, and the diameter of solder bump, have significant effects on the filling time. The physics underlying these effects is the magnitude of the resistance to flow advancement. The notion of critical design parameters, such as the critical diameter of the solder bump and the critical pitch distance, provide a bound or limit beyond which the resistance due to the constriction created by the solder bump becomes dominant in determining the filling time.

#### REFERENCES

- [1] J. Wang, "Underfill of flip-chip on organic substrate: Viscosity, surface tension, and contact angle," *Microelectron. Reliab.*, vol. 42, pp. 293–299, 2002.
- [2] D. R. Gamota and C. M. Melton, "Advanced encapsulant materials systems for flip chip on board assemblies: I. Encapsulant materials with improved manufacturing properties; II. Materials to integrate the reflow and underfilling processes," in *Proc. IEEE/CPMT Int. Electronics Manufacturing Technology Symp.*, Austin, TX, 1996, pp. 1–9.
- [3] N. W. Pascarella and D. F. Baldin, "Compression flow modeling of underfill encapsulants for low cost flip-chip assembly," *IEEE Trans. Compon., Packag. Manuf. Technol. C*, vol. 21, no. 4, pp. 325–335, Oct. 1998.
- [4] S. Han and K. K. Wang, "Analysis of the flow of encapsulant during underfill encapsulation of flip-chips," *IEEE Trans. Compon., Packag., Manuf. Technol. B*, vol. 20, no. 4, pp. 424–433, 1997.
- [5] M. K. Schwiebert and W. H. Leong, "Underfill flow as viscous flow between parallel plates driven by capillary action," *IEEE Trans. Compon., Packag., Manuf. Technol. C*, vol. 19, no. 12, pp. 133–137, Dec. 1996.
- [6] E. W. Washburn, "The dynamics of capillary flow," *Phys. Rev.*, vol. 17, pp. 273–283, 1921.
- [7] L. Nguyen, C. Quentin, P. Fine, B. Cobb, S. Bayyuk, H. Yang, and S. A. Bidstrup-Allen, "Underfill of flip-chip on laminate: Simulation and validation," *IEEE Trans. Compon. Packag. Technol.*, vol. 22, no. 2, pp. 168–176, Jun. 1999.
- [8] P. Fine, B. Cobb, and L. Nguyen, "Flip-chip underfill flow characteristics and prediction," *IEEE Trans. Compon. Packag. Technol.*, vol. 23, no. 3, pp. 420–427, Sep. 2000.
- [9] G. L. Lehmann, T. Driscoll, N. R. Guydosh, P. C. Li, and E. J. Cotts, "Underflow process for direct-chip-attachment packaging," *IEEE Trans. Compon., Packag., Manuf. Technol. A*, vol. 21, no. 2, pp. 266–274, Jun. 1998.
- [10] D. S. Kim, K. C. Lee, and T. H. Know, "Micro-channel filling flow considering surface tension effect," *J. Micromech. Microeng.*, vol. 12, pp. 236–246, 2002.
- [11] M. H. Gordon, G. Ni, W. F. Schmidt, and R. P. Selvam, "A capillary-driven underfill encapsulation process," *Adv. Packag.*, vol. 8, pp. 34–37, 1999.
- [12] R. B. Bird, W. E. Stewart, and E. N. Lightfoot, *Transport Phenomena*. New York: Wiley, 1960.
- [13] C. W. Macosko, *Rheology: Principles, Measurements, and Applications*. New York: VCH, 1994.
- [14] M. R. McNeely, M. K. Spute, N. A. Tusneem, and A. R. Oliphant, "Hydrophobic microfluidics," in *Proc. SPIE – The Int. Soc. for Optical Engineering*, vol. 3877, 1999, pp. 210–220.
- [15] M. J. Madou, *Fundamentals of Microfabrication- The Science of Miniaturization*. New York: CRC, 2002.
- [16] S. Newman, "Kinetics of wetting of surfaces by polymer: Capillary flow," *J. Colloid Interface Sci.*, vol. 26, pp. 209–213, 1968.
- [17] H. Schonhorn, H. Frisch, and T. K. Kwei, "Kinetics of wetting of surfaces by polymer melts," *J. Appl. Phys.*, vol. 37, pp. 4967–4973, 1966.
- [18] W. B. Young and W. L. Yang, "The effect of solder bump pitch on the underfill flow," *IEEE Trans. Adv. Packag.*, vol. 25, pp. 537–542, 2002.
- [19] J. W. Wan, "Theoretical and experimental investigation on a new model for calculating filling time for flip-chip underfill flow process," Tech. Rep., Dept. Mechanical Engineering, Advanced Engineering Design Lab., Univ. Saskatchewan, AEDL-JW-2004–01, 2004.



**J. W. Wan** received the M.Sc. degree in HVAC from the Xi'an University of Architecture and Technology, Xi'an, China, in 1986 and is currently pursuing the Ph.D. degree in electronic packaging at the University of Saskatchewan, Saskatoon, SK, Canada.

He was a Visiting Scholar at the Delft University of Technology, Delft, The Netherlands, from 1990 to 1991, an Associate Professor at Guangzhou University, China, from 1993 to 2000, and a Visiting Researcher in the Department of Mechanical Engineering, University of Saskatchewan, in 2001.

His current research interests include thermal control technology for electronic device and the fluid flow in microelectromechanical systems (MEMS).



**W. J. Zhang** (M'01) received the Ph.D. degree in design methodology and computer-aided design of mechanism systems from the Delft University of Technology, Delft, The Netherlands, in 1994.

He was then appointed Assistant Professor with the Department of Manufacture Engineering at the City University of Hong Kong, Hong Kong, China. In June 1998, he was appointed Associate Professor with the Department of Mechanical Engineering at the University of Saskatchewan, Saskatoon, SK, Canada, and an industrial research Chair sponsored by Atomic Energy Canada Limited (AECL) to direct the research work at the Advanced Engineering Design Laboratory (AEDL). He has been a Full Professor since July 1, 2004 with the Department of Mechanical Engineering, University of Saskatchewan. He has published (including accepted for publication) over 85 technical papers in refereed journals and numerous conference papers. His current research interests include electronics packaging design, bioengineering and biomedical engineering systems design, human-machine systems design, integrated design and control of complex systems, information modeling for design and manufacturing, and microsystems technology.

Dr. Zhang is a Member of ASME and a Senior Member of ASM.

**D. J. Bergstrom** received the Ph.D. degree in mechanical engineering from the University of Waterloo, Waterloo, ON, Canada, in 1987.

In 1987, He was appointed Assistant Professor in the Department of Mechanical Engineering at the University of Saskatchewan, Saskatoon, SK, Canada. He was promoted to Associate Professor in 1992, and Professor in 2000. As of July 1, 2004 he has been serving as Head of the Department of Mechanical Engineering. His research expertise relates to computational modeling of turbulent flows, using both Reynolds Average Navier–Stokes (RANS) models and, more recently, large eddy simulation techniques. His current research interests include experimental studies of rough-wall boundary layers, two-fluid modeling of dense solid–liquid slurry flows, and fluid flow and heat transfer in microsystems.

Dr. Bergstrom is a Member of the ASME and licensed as a Professional Engineer in the Province of Saskatchewan.